ISSN 0020-1685, Inorganic Materials, 2020, Vol. 56, No. 2, pp. 182–189. © Pleiades Publishing, Ltd., 2020.
Russian Text © The Author(s), 2020, published in Neorganicheskie Materialy, 2020, Vol. 56, No. 2, pp. 192–199.

Increasing the Sintering Rate and Strength of ZrO_2–Al_2O_3 Ceramic Materials by Iron Oxide Additions

T. O. Obolkina[a], M. A. Goldberg[a, *], V. V. Smirnov[a], S. V. Smirnov[a], D. D. Titov[a], A. A. Konovalov[a], E. A. Kudryavtsev[b], O. S. Antonova[a], S. M. Barinov[a], and V. S. Komlev[a]

[a] *Baikov Institute of Metallurgy and Materials Science, Russian Academy of Sciences, Leninskii pr. 49, Moscow, 119334 Russia*
[b] *Belgorod National Research University, ul. Pobedy 85, Belgorod, 308015 Russia*
**e-mail: mgoldberg@imet.ac.ru*

Received April 18, 2019; revised June 14, 2019; accepted July 11, 2019

Abstract—We have prepared powders and ceramic composite materials in the ZrO_2–Al_2O_3 system containing 10 and 20 wt % Al_2O_3 and examined the effect of ferric oxide additions on the linear shrinkage, phase composition, porosity, microstructure, and mechanical properties of the ZrO_2–Al_2O_3 ceramic materials. The results demonstrate that the addition of ferric oxide leads to a considerable increase in linear shrinkage and ensures porosity as low as under 1% even at a sintering temperature of 1450°C in both composite materials. Moreover, small amounts of the additive stabilize the tetragonal phase of ZrO_2, whereas increasing the Fe content to 3 mol % leads to an increase in the amount of the monoclinic phase. We have obtained densely sintered ZrO_2–10% Al_2O_3 and ZrO_2–20% Al_2O_3 ceramic materials at 1450°C, with a bending strength of up to 760 and 475 MPa, respectively.

Keywords: zirconia, alumina, oxide additive, sintering
DOI: 10.1134/S0020168520020156

INTRODUCTION

Ceramic materials based on the yttria-stabilized zirconia–alumina (YSZ–Al_2O_3) system offer unique properties: high bending strength and fracture toughness of YSZ in combination with the chemical inertness and hardness of Al_2O_3 make them widely demanded as structural and functional ceramics [1]. Such materials are used in various areas of engineering: in vital parts of machinery, the aerospace industry, medical tools, and implants [2–4]. The technology of such composite ceramics has a number of drawbacks: high sintering temperature (1600–1750°C), resulting in grain growth [5]; necessity of prolonged high-temperature heat treatment [6]; or the use of expensive processes, such as spark plasma sintering [7] or hot pressing [8].

One topical issue is the development of sintering aids based on transition metal oxides, which will make it possible to lower the sintering temperature and simplify the fabrication of YSZ–Al_2O_3 based ceramic materials. The increase in sintering rate on the addition of such sintering aids is due to the increase in the density of structural defects when heterovalent cations or cations larger than Zr^{4+} are incorporated into the YSZ lattice [9]. Of particular interest among sintering aids is ferric oxide [10, 11]. The addition of Fe_2O_3 to YSZ containing 3 and 8 mol % yttria made it possible to obtain a dense structure at a temperature of 1150°C owing to the formation of substitutional and interstitial solid solutions in the YSZ lattice, but no data were reported on the mechanical properties of the materials thus prepared. Smirnov et al. [12] demonstrated the possibility of lowering the sintering temperature of ceramics containing 5 wt % Al_2O_3 by adding ferric oxide, but grain growth prevented them from reaching good mechanical properties of the resultant materials. Raising the Al_2O_3 content helps improve the mechanical properties of composite ceramics [13]. The effect of ferric oxide on the sintering behavior of YSZ-based ceramic materials containing more than 5 wt % Al_2O_3 has not been studied previously.

The purpose of this work was to study how the concentration of ferric oxide additions influences the phase composition, sintering behavior, and mechanical properties of YSZ–Al_2O_3 ceramics containing 10 and 20 wt % Al_2O_3.

EXPERIMENTAL

ZrO_2–Al_2O_3 composite powders containing 10 and 20 wt % alumina were prepared via chemical precipitation from salt solutions. We used aqueous solutions of the $ZrOCl_2 \cdot 8H_2O$ and $AlCl_3 \cdot 6H_2O$ chlorides, which were added to a 9% aqueous ammonia. To obtain tetragonal zirconia (t-ZrO_2), yttrium chloride

($YCl_3 \cdot 6H_2O$) was added to the starting reagents to give 3 mol % yttria relative to zirconia. After the synthesis, the resultant precipitate was filtered off in a Buchner funnel, dried, and then calcined at a temperature of 650°C. The powders were mechanically activated under ethanol in a planetary mill. Ferric oxide was added in the form of the soluble salt $(NH_4)Fe(SO_4) \cdot 12H_2O$. The amount of the additive was evaluated from Fe^{3+} content: 0, 0.33, 1.0, and 3.0 mol % relative to the ZrO_2–10% Al_2O_3 and ZrO_2–20% Al_2O_3 composites. For this purpose, the as-synthesized ceramic powder was mixed with an aqueous solution containing a dissolved additive. The resultant powders were dried and passed through a 100 μm nylon sieve.

The phase composition of the powders was determined by X-ray diffraction (Difray 401 diffractometer, CrK_α radiation) using JCPDS Powder Diffraction File data and PCPDFWIN. The morphology of the synthesized powders was examined by transmission electron microscopy (TEM) on a JEOL JEM 2100 (accelerating voltage of 200 kV). Their specific surface area was determined by BET measurements (Micromeritics TriStar).

The sinterability of the materials was analyzed using dilatometry during heating to 1500°C at a rate of 10°C/min in air (Netzsch DIL 402 C). To study the properties of ceramics, the powders were pressed into beams 30 × 4 × 4 mm in dimensions. Compaction was carried out in a metallic press die set at a pressure of 100 MPa by uniaxial pressing. The resultant specimens were fired in a furnace with silit rod heaters in air.

The porosity of the ceramics was determined in accordance with the Russian Federation State Standard GOST 2409-2014. The materials were tested in three-point bending on an Instron 3382 universal testing machine. The microstructure of the ceramic materials was examined scanning electron microscopy (SEM) on a Tescan Vega II.

RESULTS AND DISCUSSION

X-ray diffraction characterization showed that, after synthesis and heat treatment at 600°C, the powders consisted of pseudocubic zirconia, c-ZrO_2 (JCPDS card no. 49-1642), with a low degree of crystallinity (Fig. 1). The X-ray diffraction patterns of the powders contained no peaks of alumina, which was due to the ability of zirconia to suppress grain growth of alumina, making it X-ray amorphous. Characteristically, the ZrO_2–20% Al_2O_3 materials had a lower intensity of reflections from c-ZrO_2 than did the ZrO_2–10% Al_2O_3 materials, which was due to the larger amount of Al_2O_3. Similar behavior of ZrO_2–Al_2O_3 composite materials heat-treated at 1000°C was reported by Balagopal et al. [1].

TEM examination of the morphology of the ZrO_2–10% Al_2O_3 powder showed that it consisted of

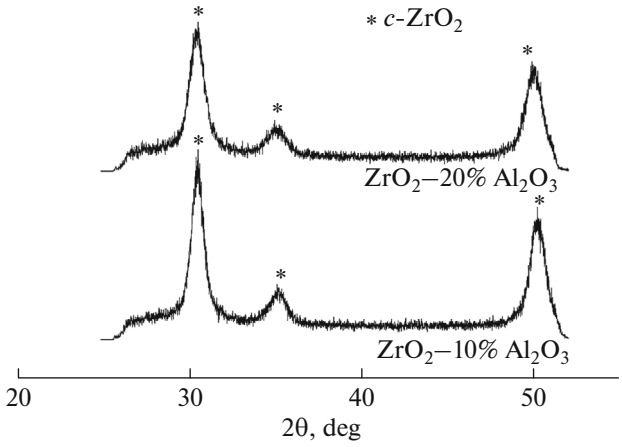

Fig. 1. X-ray diffraction patterns of the ZrO_2–10% Al_2O_3 and ZrO_2–20% Al_2O_3 powders.

rounded particles less than 10 nm in size (Fig. 2a). Raising the alumina content to 20% led to the formation of powder consisting of not only small particles, less than 10 nm in size, but also larger, faceted particles, up to 25 nm in size (Fig. 2b).

Analysis of the specific surface area (S) data showed that the addition of the lowest ferric oxide concentration to the synthesized powders caused no significant changes in their surface area. The Fe-free ZrO_2–10% Al_2O_3 composites had S = 47 m^2/g. The addition of ferric oxide led to changes in specific surface by no more than 5%, independent of its concentration. The ZrO_2–20% Al_2O_3 materials had a larger specific surface area, 54 m^2/g, which was probably due to the lower degree of aggregation of the powders. The ferric oxide-containing powders also had S in the range 50–55 m^2/g.

According to the dilatometry data, the addition of even the lowest ferric oxide concentration (0.33 mol % Fe^{3+}) to the composite materials of the ZrO_2–Al_2O_3 system significantly improved their sinterability (Fig. 3). In the case of the ZrO_2–10% Al_2O_3 materials, a well-defined effect was observed on the addition of 0.33 mol % Fe, which increased the shrinkage of the samples from 13.8 (with no additive) to 24.1%. The first stage of sintering, at temperatures in the range 900–950°C, was shown to be associated with the phase transition from the monoclinic phase of ZrO_2 (m-ZrO_2) to the tetragonal phase (t-ZrO_2). The onset of an active sintering process, associated with the heat-treatment-induced densification of the material, was observed at a temperature of 1010°C. Raising the ferric oxide content of the ZrO_2–10% Al_2O_3 samples led to an increase in linear shrinkage to 26.2%. The materials underwent considerable densification in the temperature range 1320–1350°C.

Increasing the alumina content of the materials had a negative effect on their sinterability. In particu-

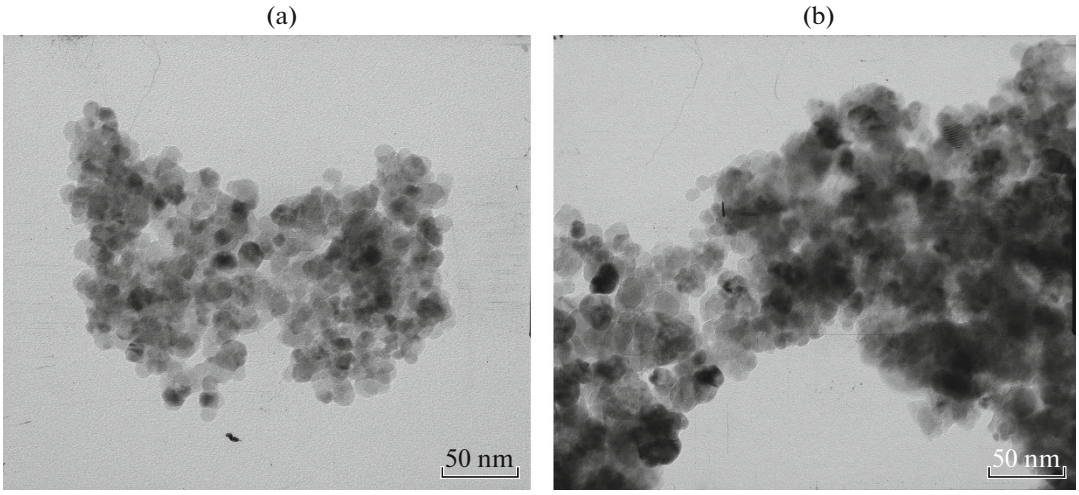

Fig. 2. TEM micrographs of the (a) ZrO_2–10% Al_2O_3 and (b) ZrO_2–20% Al_2O_3 powders.

lar, the Fe-free ZrO_2–20% Al_2O_3 samples showed a linear shrinkage of 7.5%. The addition of 0.33 mol % Fe^{3+} increased the shrinkage to 10.0%. Raising the Fe^{3+} content to 3 mol % lead to further increase in shrinkage, up to 13.3%.

According to X-ray diffraction data, the Fe-free ZrO_2–10% Al_2O_3 materials sintered at 1450°C contained *t*-ZrO_2 (JCPDS card no. 42-1164) and a small amount of the *m*-ZrO_2 phase (JCPDS card no. 37-1484), within 5 wt %. The amount of this phase increased as the sintering temperature was raised to 1500°C (Figs. 4a, 4b). Al_2O_3 crystallized in the form of corundum (JCPDS card no. 10-0173).

The addition of 0.33 or 1.0 mol % Fe to the ZrO_2–10% Al_2O_3 composite materials led to an increase in the amount of *t*-ZrO_2, whereas *m*-ZrO_2 almost completely disappeared (Fig. 4). Increasing the amount of the additive to 3 mol % led to the formation of up to 20 wt % *m*-ZrO_2, whereas the intensity of the reflections from Al_2O_3 remained essentially unchanged. Raising the sintering temperature to 1500°C led to an increase in *m*-ZrO_2 content to 40% as the amount of the additive was increased to 3 mol % Fe^{3+}. Note that the addition of 3 mol % Fe^{3+} eliminated the splitting of the peaks at $2\theta = 49.46°$ and 50.06° to give a single peak at 50.22°, characteristic of *c*-ZrO_2.

The oxide-additive-free ZrO_2–20% Al_2O_3 samples are characterized by the formation of up to 10 and 20 wt % *m*-ZrO_2 at 1450 and 1500°C, respectively (Figs. 4c, 4d). The addition of 0.33 or 1.0 mol % Fe^{3+} stabilizes *t*-ZrO_2, whereas the addition of 3 mol % Fe^{3+} leads to an increase in the amount of *m*-ZrO_2 and eliminates the doublet in the range 49.8°–51.2° to give a single peak characteristic of *c*-ZrO_2, at both 1450 and 1500°C.

The measured porosity data for our samples are presented in Table 1. All of the ZrO_2–10% Al_2O_3 samples containing additives were shown to be densely sintered, with a porosity under 1% even at 1450°C. The additive-free materials were characterized by a 7.7% porosity at a sintering temperature of 1450°C. The additive-free ZrO_2–20% Al_2O_3 materials sintered at 1450°C had higher porosity, up to 18.55%. The addition of 3 mol % Fe^{3+} to ZrO_2–20% Al_2O_3 allowed a densely sintered state to be reached. Both the ZrO_2–10% Al_2O_3 and ZrO_2–20% Al_2O_3 materials heat-treated at 1500°C were in a densely sintered state.

Figure 5 illustrates the microstructure of the ZrO_2–10% Al_2O_3 ceramics containing 0, 0.33, 1.0, and 3.0 mol % Fe and sintered at 1450°C. The ceramics have a dense microstructure. Characteristically, the additive-free materials have a nonuniform microstructure made up of fine grains, 0.1–0.3 μm in size, and larger grains, 1.0–2.0 μm in size. Alumina in the form of dark grains is uniformly distributed over the material in the form of agglomerates up to 0.5 μm in size. The addition of 0.33 mol % Fe^{3+} leads to an increase in the size of the fine grains, which reaches 0.5–0.7 μm, and an increase in the number of large crystals, up to 50% of the field of view. In the structure of the ceramic containing 1 mol % Fe^{3+}, we observe further recrystallization, resulting in the formation of large, irregularly shaped grains ranging in size from 2.0 to 3.0 μm. At 3 mol % Fe^{3+}, the large grains account for up to 70% of the field of view and are a predominant phase. The microstructure of the ZrO_2–10% Al_2O_3 ceramic containing 3 mol % Fe is made up of sintered large grains, ranging in size from 1.5 to 3 μm; intermediate grains (0.5 to 1 μm in size), and fine grains (0.3 μm).

The ZrO_2–20% Al_2O_3 ceramics containing different amounts of ferric oxide and sintered at 1450°C

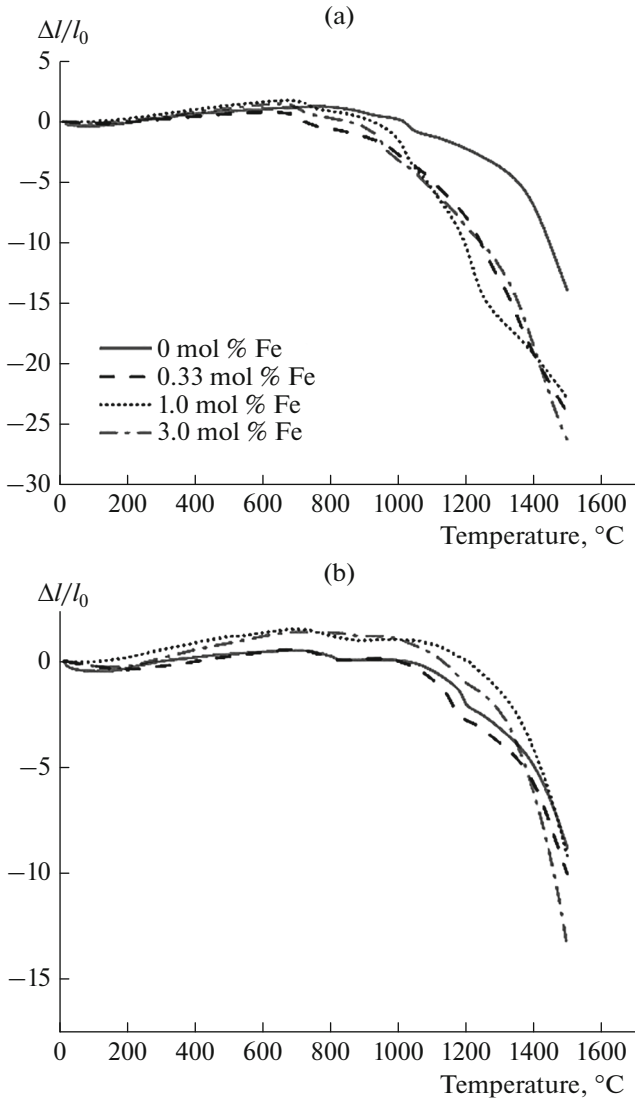

Fig. 3. Shrinkage curves of the (a) ZrO_2–10% Al_2O_3 and (b) ZrO_2–20% Al_2O_3 materials from dilatometry data.

have a similar microstructure (Fig. 6). The ZrO_2–20% Al_2O_3 ceramics containing 0.33 mol % Fe^{3+} have a uniform microcrystalline structure ranging in grain size from 0.1 to 0.5 μm. Increasing the ferric oxide content leads to the formation of large, sintered grains 2 μm in size, while the grains less than 0.5 μm in size also persist. We observe accumulations of alumina grains (dark grains) up to 1 μm in size. The alumina grain agglomerates are uniformly distributed over the entire field of view.

The addition of Fe^{3+} led to a significant increase in the strength of the sintered ZrO_2–10% Al_2O_3 ceramic materials (Fig. 7). The additive-free materials sintered at 1450°C were characterized by an average strength of 530 MPa. Reaching a densely sintered state at 1450°C and stabilizing t-ZrO_2 in the materials containing

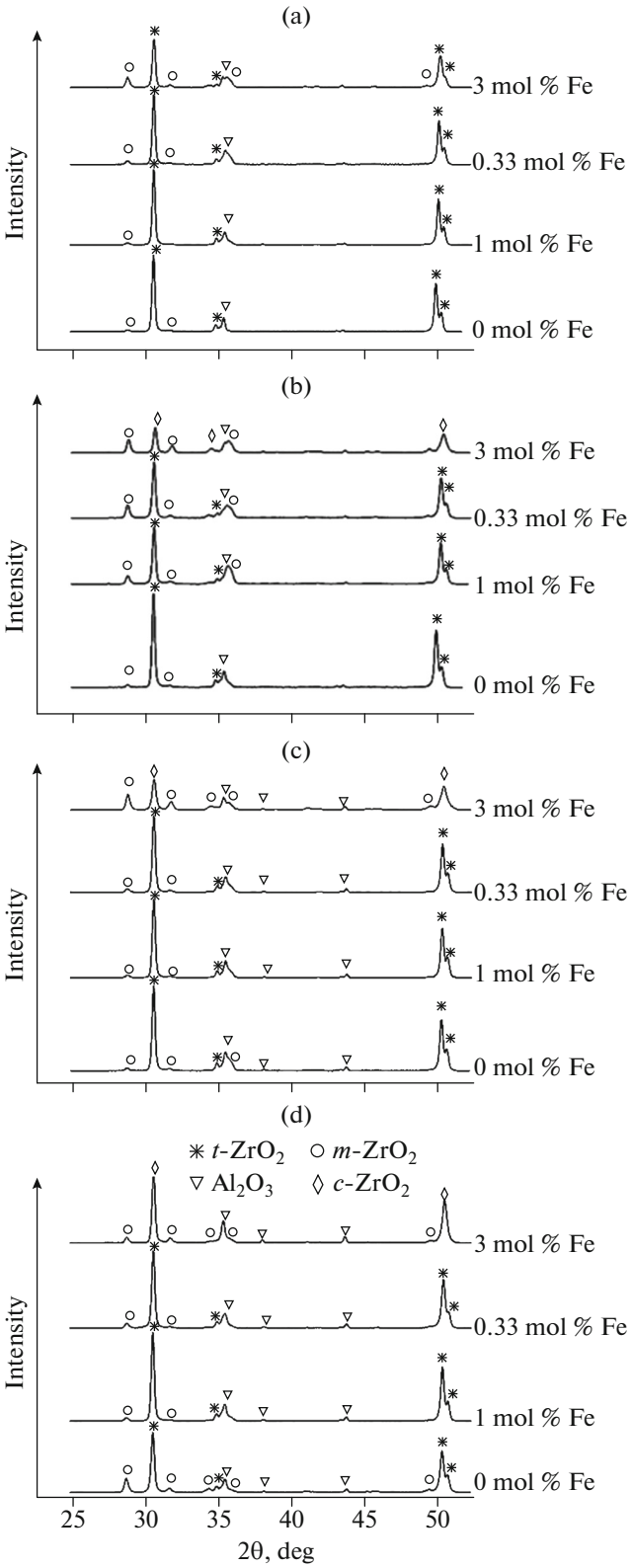

Fig. 4. X-ray diffraction patterns of the (a, b) ZrO_2–10% Al_2O_3 and (c, d) ZrO_2–20% Al_2O_3 ceramics prepared by sintering at (a, c) 1450 and (b, d) 1500°C.

Table 1. Influence of the composition and sintering temperature of the materials on their porosity

Composition	Sintering temperature, °C	Porosity, %
ZrO_2–10% Al_2O_3	1450	7.77
ZrO_2–10% Al_2O_3–0.33% Fe		0.82
ZrO_2–10% Al_2O_3–1% Fe		0.75
ZrO_2–10% Al_2O_3–3% Fe		0.02
ZrO_2–10% Al_2O_3	1500	0.29
ZrO_2–10% Al_2O_3–0.33% Fe		0.61
ZrO_2–10% Al_2O_3–1% Fe		0.54
ZrO_2–10% Al_2O_3–3% Fe		0.18
ZrO_2–20% Al_2O_3	1450	18.55
ZrO_2–20% Al_2O_3–0.33% Fe		12.26
ZrO_2–20% Al_2O_3–1% Fe		5.61
ZrO_2–20% Al_2O_3–3% Fe		0.47
ZrO_2–20% Al_2O_3	1500	0.19
ZrO_2–20% Al_2O_3–0.33% Fe		0.41
ZrO_2–20% Al_2O_3–1% Fe		0.2
ZrO_2–20% Al_2O_3–3% Fe		0.68

0.33 mol % Fe^{3+} allowed the strength in three-point bend tests to reach 760 ± 25 MPa. Further raising Fe_2O_3 content to 1.0 and 3.0 mol % led to a reduction in strength to 710 ± 20 and 600 ± 20 MPa, respectively, which was due to the formation of a large-grained microstructure and the phase transition of *t*-ZrO_2 to *m*-ZrO_2. Raising the sintering temperature to 1500°C led on average to a decrease in strength in three-point bend tests because of the formation of monoclinic phase in the additive-free materials and the increase in its content in the Fe-containing materials. Moreover, the increase in sintering temperature led to ceramic grain growth, thereby impairing the mechanical properties of the ceramics [5].

The ZrO_2–20% Al_2O_3 sample sintered at 1450°C had lower strength than did the ZrO_2–10% Al_2O_3 materials because they retained porosity (Fig. 8). In particular, the strength of the additive-free materials was 320 ± 15 MPa, whereas the addition of 1.0 mol % Fe^{3+} led to an increase in strength to 475 ± 20 MPa. The strength of the materials containing 3.0 mol % Fe^{3+} did not exceed 350 MPa, even though their porosity was under 1%. X-ray diffraction results sug-

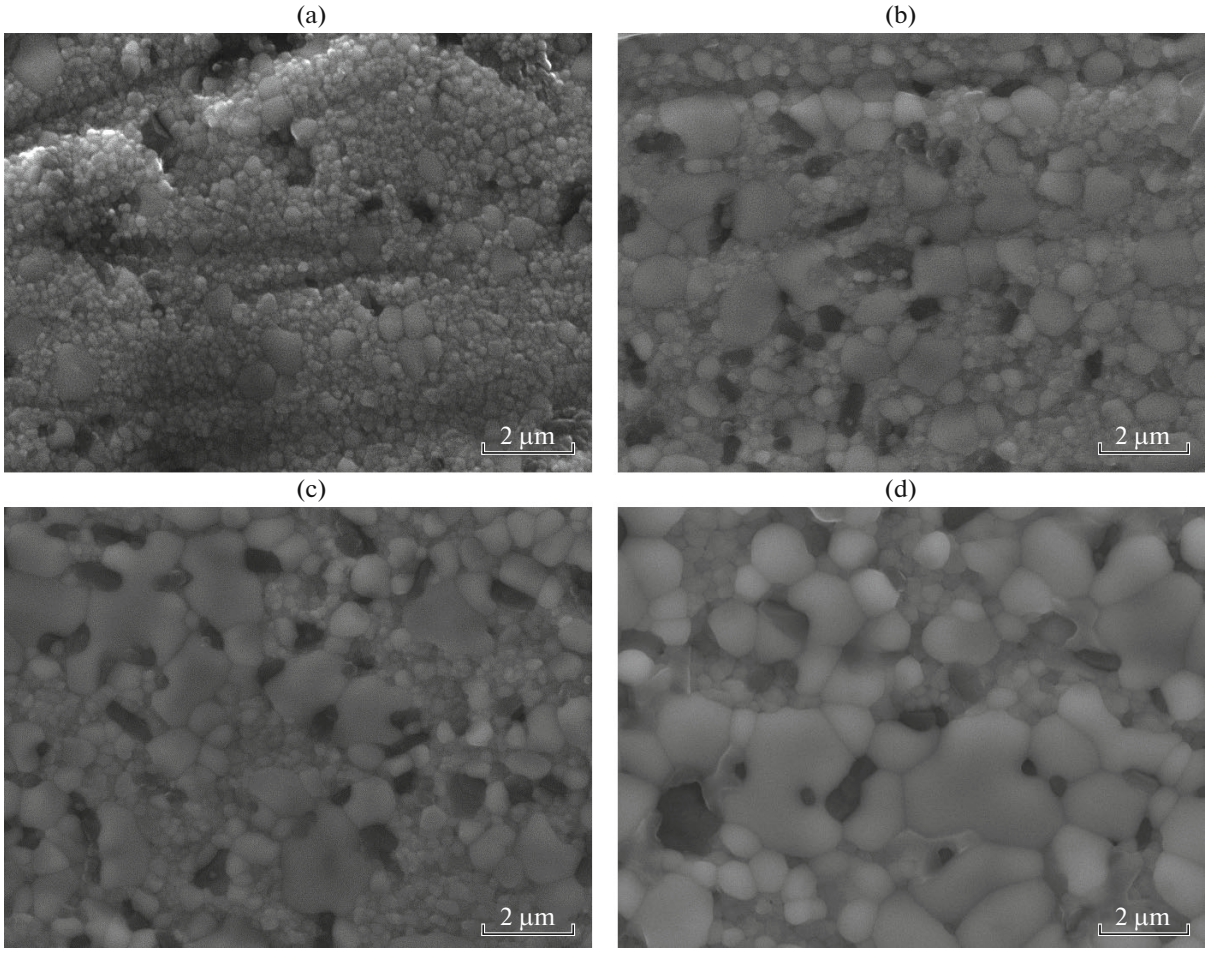

Fig. 5. Microstructure of the ZrO_2–10% Al_2O_3 ceramics containing (a) 0, (b) 0.33, (c) 1.0, and (d) 3.0 mol % Fe and sintered at 1450°C.

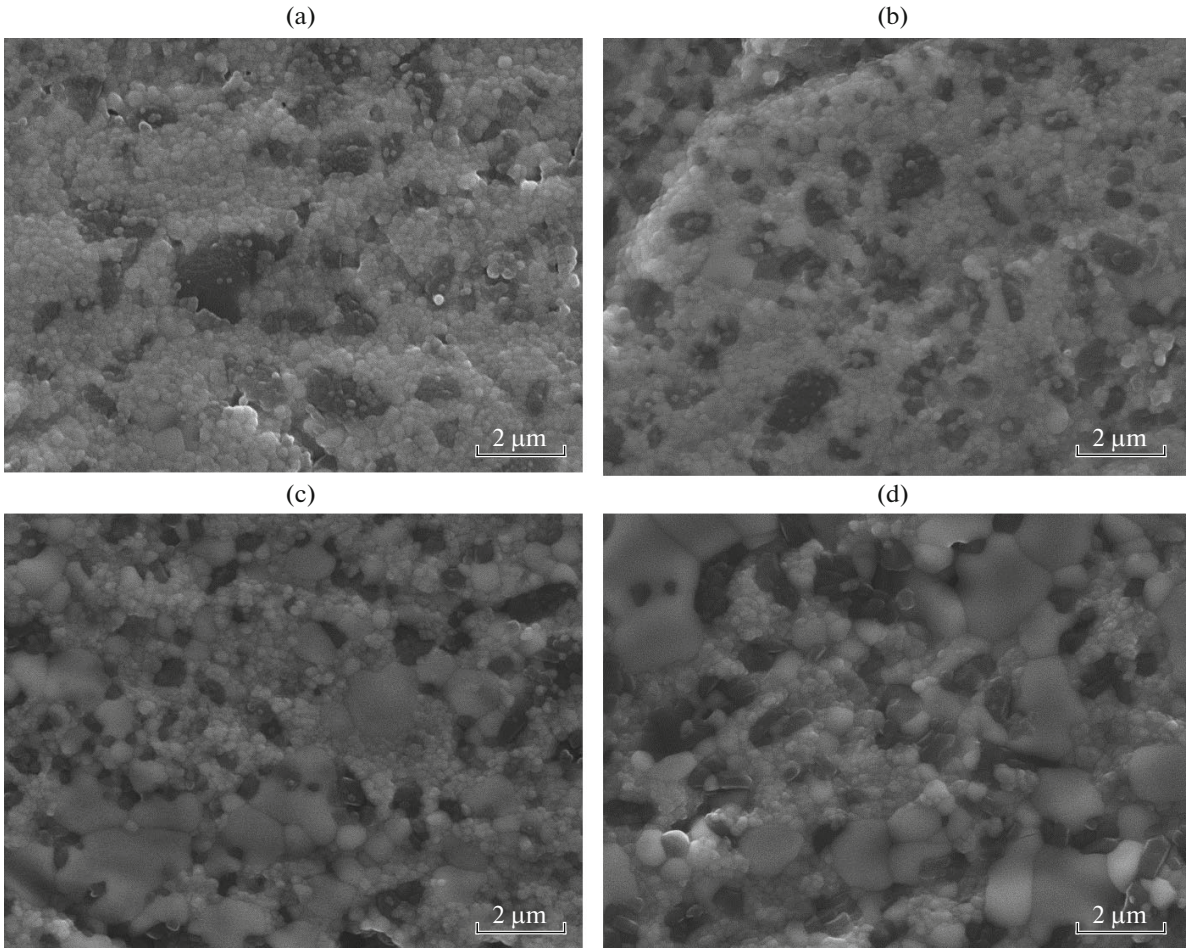

Fig. 6. Microstructure of the ZrO_2–20% Al_2O_3 ceramics containing (a) 0, (b) 0.33, (c) 1.0, and (d) 3.0 mol % Fe and sintered at 1450°C.

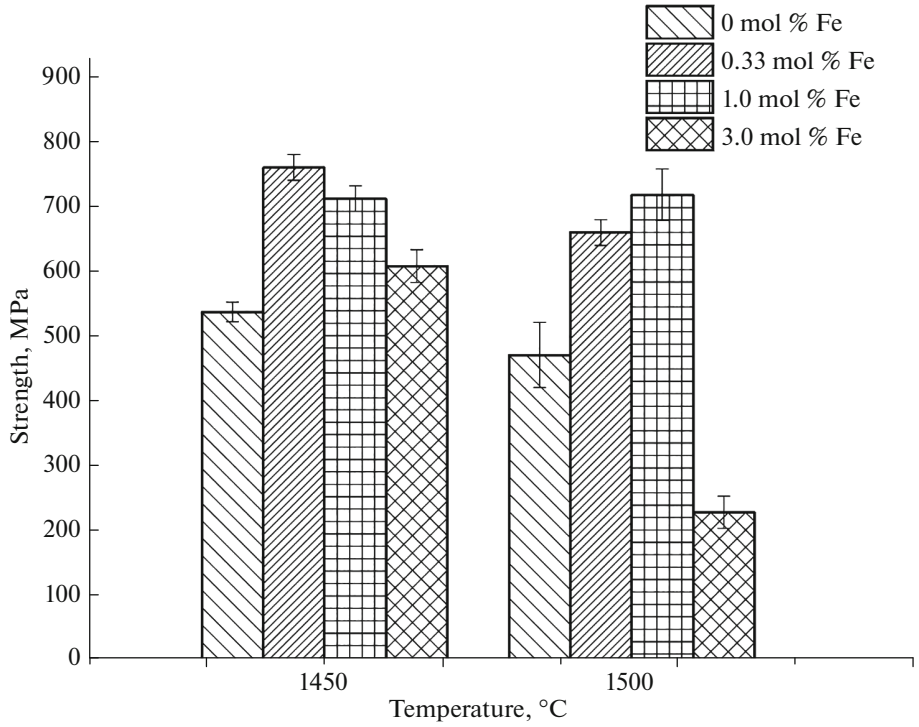

Fig. 7. Effects of composition and sintering temperature on the strength of the ZrO_2–10% Al_2O_3 ceramics.

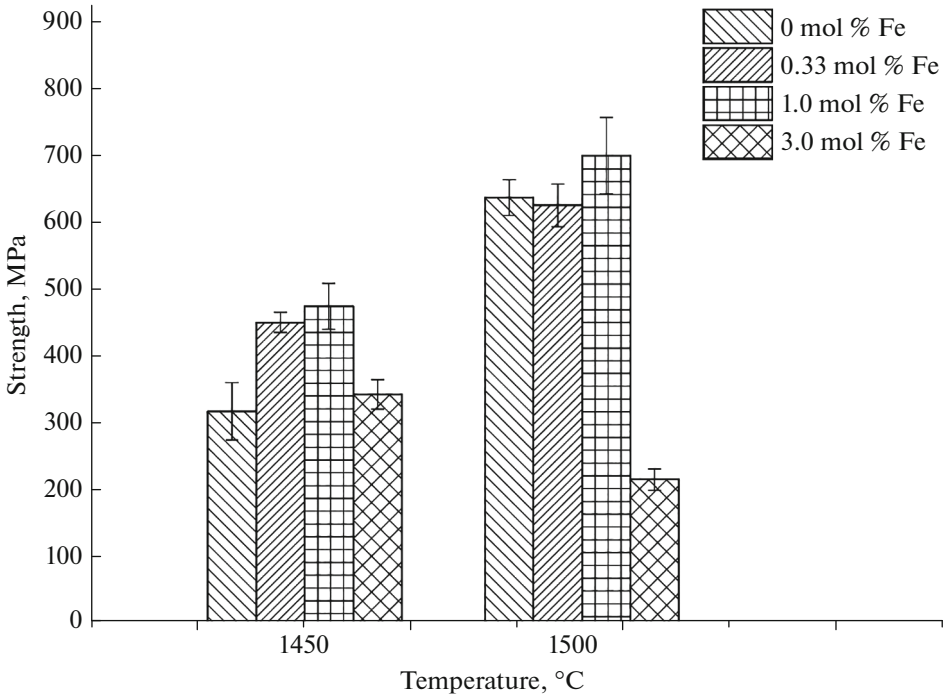

Fig. 8. Effects of composition and sintering temperature on the strength of the ZrO_2–20% Al_2O_3 ceramics.

gested that this was due to the considerable concentration of *m*-ZrO_2, a low-strength phase. Raising the sintering temperature to 1500°C made it possible to reach a densely sintered state in all of the samples and an average strength near 700 MPa for the sample containing 1.0 mol % Fe. This sample was characterized by the largest amount of *t*-ZrO_2, a high-strength phase. The average strength of the additive-free material was 630 ± 15 MPa.

CONCLUSIONS

The addition of ferric oxide has been shown to cause a considerable increase in the linear shrinkage of the materials containing 10 and 20 wt % Al_2O_3. The addition of 0.33–1.0 mol % Fe^{3+} helps stabilize the tetragonal phase of zirconia, whereas the addition of 3 mol % Fe^{3+} stabilizes *m*-ZrO_2 and leads to appreciable ceramic grain growth. We have obtained densely sintered ZrO_2–10% Al_2O_3 ceramic materials at 1450°C and Fe^{3+}-containing ZrO_2–20% Al_2O_3 ceramics at 1500°C. The addition of ferric oxide during sintering at 1450°C for 2 h has allowed the strength of the materials in three-point bend tests to be raised by 45–50%: to 760 MPa for the ZrO_2–10% Al_2O_3 composite materials and to 475 MPa for the ZrO_2–20% Al_2O_3 composites.

FUNDING

This work was supported by the Russian Federation President's Grant no. MK-5661.2018.8 and the Russian Federation President's Scholarship no. SP-3724.2018.4.

REFERENCES

1. Balagopal, N., Warrier, K.G.K., and Damodaran, A.D., Alumina–ceria composite powders through a flash combustion technique, *J. Mater. Sci. Lett.,* 1991, vol. 10, no. 19, pp. 1116–1118.
2. Deshmukh, R.M. and Kulkarni, S.S., A review on biomaterials in orthopedic bone plate application, *Int. J. Current Eng. Technol.,* 2015, vol. 5, no. 4, pp. 2587–2591.
3. Nevarez-Rascon, A., Gonzalez-Lopez, S., Acosta-Torres, L.S., Nevarez-Rascon, M.M., and Orrantia-Borunda, E., Synthesis, biocompatibility and mechanical properties of ZrO_2–Al_2O_3 ceramics composites, *Dental Mater. J.,* 2016, vol. 35, no. 3, pp. 392–398.
4. Smirnov, V.V., Krylov, A.I., Smirnov, S.V., Goldberg, M.A., Antonova, O.S., Kochanov, G.P., and Barinov, S.M., Sintering and microstructure of materials based on the fluorohydroxyapatite–ZrO_2–Al_2O_3 system, *Inorg. Mater.,* 2016, vol. 52, no. 10, pp. 1025–1030.
5. Matsui, K., Ohmichi, N., Ohgai, M., Yoshida, H., and Ikuhara, Y., Effect of alumina-doping on grain boundary segregation-induced phase transformation in yttria-stabilized tetragonal zirconia polycrystal, *J. Mater. Res.,* 2006, vol. 21, no. 9, pp. 2278–2289.
6. Jayaseelan, D., Nishikawa, T., Awaji, H., and Gnanam, F.D., Pressureless sintering of sol–gel derived

alumina–zirconia composites, *Mater. Sci. Eng., A,* 1998, vol. 256, nos. 1–2, pp. 265–270.

7. Akin, I., Yilmaz, E., Sahin, F., Yucel, O., and Goller, G., Effect of CeO_2 addition on densification and microstructure of Al_2O_3–YSZ composites, *Ceram. Int.,* 2011, vol. 37, no. 8, pp. 3273–3280.
8. Xu, X., Xu, X., Liu, J., Hong, W., and Hou, F., Low-temperature fabrication of Al_2O_3–ZrO_2 (Y_2O_3) nanocomposites through hot pressing of amorphous powders, *Ceram. Int.,* 2016, vol. 42, no. 13, pp. 15 065–15 071.
9. Flegler, A.J., Burye, T.E., Yang, Q., and Nicholas, J.D., Cubic yttria stabilized zirconia sintering additive impacts: a comparative study, *Ceram. Int.,* 2014, vol. 40, no. 10, pp. 16 323–16 335.
10. Foschini, C.R., Souza, D.P.F., Paulin Filho, P.I., and Varela, J.A., AC impedance study of Ni, Fe, Cu, Mn doped ceria stabilized zirconia ceramics, *J. Eur. Ceram. Soc.*, 2001, vol. 21, no. 9, pp. 1143–1150.
11. Guo, F. and Xiao, P., Effect of Fe_2O_3 doping on sintering of yttria-stabilized zirconia, *J. Eur. Ceram. Soc.,* 2012, vol. 32, no. 16, pp. 4157–4164.
12. Smirnov, V.V., Obolkina, T.O., Krylov, A.I., Smirnov, S.V., Goldberg, M.A., Antonova, O.S., and Barinov, S.M., Agglomeration and properties of ceramics based on partially stabilized zirconium dioxide containing oxides of aluminum and iron, *Inorg. Mater.: Appl. Res.,* 2018, vol. 9, no. 1, pp. 121–124.
13. Ye, Y., Li, J., Zhou, H., and Chen, J., Microstructure and mechanical properties of yttria-stabilized ZrO_2/Al_2O_3 nanocomposite ceramics, *Ceram. Int.,* 2008, vol. 34, no. 8, pp. 1797–1803.

Translated by O. Tsarev